This is an electronic appendix to the paper by Lloyd-Smith *et al*. 2003 Curtailing transmission of severe acute respiratory syndrome within a community and its hospital. *Proc. R. Soc. Lond.* B **270**, 1979–1989. (DOI 10.1098/rspb.2003.2481.)

Electronic appendices are refereed with the text. However, no attempt has been made to impose a uniform editorial style on the electronic appendices.

Electronic appendix A

Sensitivity to population size

We tested the sensitivity of key model results to both absolute and relative changes in pool sizes. Figure S1 shows results obtained when both pools are reduced ten-fold in size (i.e. for a HCW pool of 300 individuals, and community pool of 10,000). Comparing these figures to those in the main text, we see that changes in system scale do not qualitatively alter our findings. This is not surprising, since we treat contact rates as density-independent and restrict our attention to the invasion phase when overall prevalence is less than 1%.

It is less clear whether our results will be sensitive to changes in the relative size of the two pools, since this will alter the weighting of different transmission pathways. In Figure S2 we present the same analyses when the HCW pool contains 1000 individuals (compared to 3000 throughout the main text), and community pool is still 100,000 individuals. Results pertaining to the reproductive number (Figs S2A-B) are not significantly changed, again due to our assumption of density-independent contact rates. When the evolving epidemic is simulated, though, slight differences emerge. A smaller HCW pool seems to slightly extend the window of time within which the combined control strategy contributes to outbreak containment (Fig. S2C), perhaps due to slower initial spread. This effect is subtle but persists in all our simulations. The possibility that smaller hospital size reduces the risk of outbreaks is intriguing and has implications for health policy, and merits further investigation. In Figure S2D we see some changes in proportional routes of transmission, but the essential result remains that reducing HCW-community contacts can prevent leakage of the infection from the hospital.

Robustness of transmission-reduction results

A major finding of this study is that hospital-oriented contact precautions, such as wearing masks and gowns at all times and respiratory isolation of identified patients, are the most potent measures for combating an incipient SARS outbreak. Figures S1B and S2B show that this conclusion is robust to absolute and relative changes in pool sizes. We now explore the sensitivity of this result to different case management scenarios and R_0 values, by plotting analogues of Figure 2F to show the effect of each transmission-reduction parameter on R.

We first consider a scenario with no quarantining (Fig. S3A), which leads to a greater proportion of symptomatic individuals spending their initial days of symptoms mixing freely with the community. This reduces the contribution of hospital-based transmission to R, and accordingly we see a smaller relative contribution of η and κ to determining the effective reproductive

number. Reinforcing this point, a scenario with less efficient case isolation and no quarantining (Fig. S3B) exhibits still weaker dependence of R on the values of η and κ, and thus greater relative sensitivity to ρ. The three measures are almost equivalent as the parameters approach zero—we see that stopping HCW-community transmission ($\rho \to 0$) has a roughly equal effect to perfect case isolation ($\kappa \to 0$) and almost as great an effect as eliminating within-hospital transmission entirely ($\eta \to 0$). Strikingly, though, note that the cost of poor hospital-wide contact precautions ($\eta \to 1$) is much greater now that the rate of isolating symptomatic HCWs is low. Indeed, the adverse effect of $\eta \to 1$ is always higher than any other failure of transmission-control measures. Some degree of hospital-wide contact precautions is thus essential to combating a SARS outbreak.

Finally, considerating the original case management strategy but raising R_0 to 5 (Fig. S3C) shows that the overall transmissibility acts only to scale the lines from Figure 2F, but does not alter their relation to one another.

Model equations

For ease of presentation, the following equations show a deterministic analogue of our model. All terms shown here as products of a probability and a state variable are generated in our simulations by drawing binomial random variables. The community pool is described as follows, where all variables and parameters are as described in Figure 1 of the main text:

$$S_c(t+1) = \exp\big(-\lambda_c(t)\big) S_c(t)$$
$$E_{c,1}(t+1) = \big[1 - \exp\big(-\lambda_c(t)\big)\big] S_c(t)$$
$$E_{c,i}(t+1) = (1-p_{i-1})(1-q_{i-1}) E_{c,i-1}(t) \qquad i = 2,\ldots,10$$
$$I_{c,1}(t+1) = \sum_{i=1}^{10} p_i (1-q_i) E_{c,i}(t)$$
$$I_{c,2}(t+1) = (1-h_{c,1}) I_{c,1}(t)$$
$$I_{c,3}(t+1) = (1-h_{c,2}) I_{c,2}(t) + (1-r)(1-h_{c,3}) I_{c,3}(t)$$
$$I_{c,j}(t+1) = r(1-h_{c,j-1}) I_{c,j-1}(t) + (1-r)(1-h_{c,j}) I_{c,j}(t) \quad j = 4,5$$
$$R_c(t+1) = R_c(t) + r I_{c,5}(t) + \big[r I_{m,5}(t)\big]^*$$

Daily probabilities of quarantine (q_i) or hospitalization ($h_{c,i}$) are subscripted by i because they can vary between subcompartments (in the analysis presented here they vary only between 0 and a fixed value, to describe delays in contact tracing or case identification). The final term in the $R_c(t+1)$ equation is marked with an asterisk because only those individuals in $I_{m,5}$ who were originally from the community pool (i.e. community members who have been hospitalized) move to the R_c pool upon their recovery. Individuals in $I_{m,5}$ who began in the HCW pool progress to R_h upon recovery (indicated below with another asterisk). The equations for the HCW pool are:

$$S_h(t+1) = \exp\big(-\lambda_h(t)\big)S_h(t)$$
$$E_{h,1}(t+1) = \big[1-\exp\big(-\lambda_h(t)\big)\big]S_h(t)$$
$$E_{h,i}(t+1) = (1-p_{i-1})E_{h,i-1}(t) \qquad i = 2,...,10$$
$$I_{h,1}(t+1) = \sum_{i=1}^{10} p_i(1-q_i)E_{h,i}(t)$$
$$I_{h,2}(t+1) = (1-h_{h,1})I_{h,1}(t)$$
$$I_{h,3}(t+1) = (1-h_{h,2})I_{h,2}(t) + (1-r)(1-h_{h,3})I_{h,3}(t)$$
$$I_{h,j}(t+1) = r(1-h_{h,j-1})I_{h,j-1}(t) + (1-r)(1-h_{h,j})I_{h,j}(t) \quad j = 4,5$$
$$R_h(t+1) = R_h(t) + rI_{h,5}(t) + \big[rI_{m,5}(t)\big]^*$$

As described in the caption of Figure 1 (main text), the total hazard rates are $\lambda_c=[\beta(I_c+\varepsilon E_c)+ \rho\beta(I_h+\varepsilon E_h)+\gamma\beta\varepsilon E_m]/N_c$ and $\lambda_h=\rho\lambda_c+\eta\beta(I_h+\varepsilon E_h+\kappa I_m)/N_h$, where E_j and I_j represent sums over all sub-compartments in the incubating and symptomatic classes for pool j. The effective number of individuals in the hospital mixing pool is $N_h=S_h+E_h+I_h+R_h+I_m$, and in the community mixing pool is $N_c=S_c+E_c+I_c+R_c+ \rho(S_h+E_h+I_h+R_h)$. In simulations, the number of infection events in each timestep is determined by random draws from binomial(S_j, $1-exp(-\lambda_j)$) distributions ($j=c,h$).

Finally, the equations describing the case-managed pool (quarantined and case-isolated individuals) are as follows:

$$E_{m,i}(t+1) = (1-p_{i-1})\big[q_{i-1}E_{c,i-1}(t) + E_{m,i-1}(t)\big] \qquad i = 2,...,10$$
$$I_{m,1}(t+1) = \sum_{i=1}^{10} p_i\big[q_iE_{c,i}(t) + E_{m,i}(t)\big]$$
$$I_{m,2}(t+1) = h_{c,1}I_{c,1}(t) + h_{h,1}I_{h,1}(t) + I_{m,1}(t)$$
$$I_{m,3}(t+1) = h_{c,2}I_{c,2}(t) + h_{h,2}I_{h,2}(t) + I_{m,2}(t) + (1-r)\big[h_{c,3}I_{c,3}(t) + h_{h,3}I_{h,3}(t) + I_{m,1}(t)\big]$$
$$I_{m,j}(t+1) = r\big[h_{c,j-1}I_{c,j-1}(t) + h_{h,j-1}I_{h,j-1}(t) + I_{m,j-1}(t)\big] + (1-r)\big[h_{c,j}I_{c,j}(t) + h_{h,j}I_{h,j}(t) + I_{m,j}(t)\big] \quad j = 4,5$$

Calculation of the reproductive number

The progression of each infected individual through incubating and symptomatic stages of the disease, and possibly through case management stages, can be described by a stochastic transition matrix. When the removed state is included, the infectious lifetime of each individual can be represented as an absorbing Markov chain (where "absorption" corresponds to the end of the infectious period). For a given set of transition probabilities (i.e. disease progression parameters and probabilities of entering case management from each disease stage), the expected residence time in each pre-absorption stage can be calculated from the fundamental matrix of the Markov chain (Caswell 2000).

Since case management probabilities may vary between the community and hospital pools, we define d_j (for $j=c$ or h) as a vector of expected residence times in the states (E_j,I_j,E_m,I_m), i.e. the length of time a "typical" individual infected in pool j will spend in each of those disease classes. We the define b_{jk} as vectors of transmission rates from pool j to pool k for each disease state. In particular, from the above description we have

$b_{cc}=(\varepsilon\beta/N_c,\beta/N_c,\gamma\varepsilon\beta/N_c,0)$,
$b_{ch}=(\rho\varepsilon\beta/N_c,\rho\beta/N_c,\rho\gamma\varepsilon\beta/N_c,\kappa\eta\beta/N_h)$,
$b_{hc}=(\rho\varepsilon\beta/N_c,\rho\beta/N_c,\gamma\varepsilon\beta/N_c,0)$, and
$b_{hh}=(\rho^2\varepsilon\beta/N_c+\eta\varepsilon\beta/N_h,\rho^2\beta/N_c+\eta\beta/N_h,\rho\gamma\varepsilon\beta/N_c,\kappa\eta\beta/N_h)$.

The two terms in the first two elements of b_{hh} represent community and workplace exposure risks for healthcare workers, respectively. The factors of ρ^2 reflect that community transmission between HCWs depends on the community-contact precautions of both HCWs.

For a susceptible individual in pool k, the total hazard of infection due to the index case is thus $\lambda_{jk}=d_j\cdot b_{jk}$, so the probability of exposure is $1-\exp(-\lambda_{jk})$. If there are S_k susceptibles in pool k, then the expected number of secondary infections in pool k due to an index case who is infected in pool j is $R_{jk}=[1-\exp(-\lambda_{jk})]S_k$. We then define the next-generation matrix:

$$\mathbf{R}=\begin{bmatrix} R_{cc} & R_{ch} \\ R_{hc} & R_{hh} \end{bmatrix}$$

where the individual elements R_{ij} give insight into the potential for disease spread within and between the two pools. If **R** is primitive, then its dominant eigenvalue is the reproductive number for the entire system (Diekmann & Heesterbeek 2000). When the population is entirely susceptible and no control measures are in place this is the basic reproductive number, R_0; otherwise it is the effective reproductive number R. Figure 2A of the main text shows the probability of epidemic containment as a function of the reproductive number, which displays the qualitative behaviour expected for a stochastic epidemic: the probability is nearly one for $R<1$, then diminishes as R increases (but remains significantly greater than zero up to $R\sim5$).

Incubation and symptomatic periods

The incubation period is modeled with ten subcompartments as shown in Figure 1B of the main text. Each sub-compartment represents one day, and an individual in their i^{th} day since infection has a probability p_i of progressing to the symptomatic phase of the disease. The number of sub-compartments and values of p_i were chosen to be consistent with clinical data from 42 patients in Toronto with a single known contact with a SARS case. For these cases, the mean incubation period was 5 days, with a median of 4 days and a range from 2 to 10 days (Health Canada 2003); similar numbers are reported for 21 point-exposure cases in Singapore (Leo et al. 2003). We selected the most parsimonious model which was consistent with these data: 10 subcompartments with p_i interpolated linearly from $p_1=0$ to $p_{10}=1$. Figure S4A shows the distribution of incubation periods obtained from this model, which has a mean period of 4.5 days, a median period of 4 days, and a range from 2 to 10 days. Other researchers have

presented a distribution of incubation periods which includes longer durations (Donnelly et al. 2003), but experts assembled by the World Health Organization continue to assert a maximum incubation period of 10 days (World Health Organization 2003b).

The symptomatic period is modeled with two disease-age subcompartments and three disease-stage subcompartments. After each day individuals automatically progress through the age sub-compartments, and progress through the stage subcompartments with probability r. We include the initial disease-age subcompartments to allow assessment of the importance of beginning case isolation following day 1, 2 or 3 of symptoms. We assume that individuals are symptomatic for at least 5 days. From clinical reports of 23 patient histories we estimated that the distribution of symptomatic period has a mean of 16.2 days (with standard deviation of 7.9 days) and a median 16 days (Poutanen et al. 2003, Tsang et al. 2003). Figure S4B shows the distribution of symptomatic periods obtained from our model (with r=0.21), which has a mean period of 16.3 days, a median period of 15 days, and a standard deviation of 7.3 days.

While our modelled distribution is roughly consistent with data, we note that estimation of the symptomatic period poses a difficult challenge. We are seeking to capture the period of high infectiousness (which we call the symptomatic period to distinguish it from the incubation period, during which we assume individuals may be slightly infectious), but this is difficult to gauge because infectiousness is not readily observable. Our estimated symptomatic period—or highly infectious period—falls between those used in the two first modelling analyses of SARS outbreaks. Riley et al (2003) use hospitalization periods as a surrogate, and present a range of mean symptomatic periods from 27 to 41 days. (These include a symptomatic, not-yet-hospitalized period with mean duration of 3.67-4.84 days, and a symptomatic, hospitalized period with mean duration of 23.5 or 35.9 days depending on clinical outcome. Transmission by hospitalized individuals is reduced by a factor of 0.2, analogous to our κ.) Lipsitch et al (2003) do not model the symptomatic period directly but instead assume an "average duration of infectiousness" of 5 days (range: 1-5 days). This is markedly shorter than the symptomatic periods used in our model (and that of Riley et al), but the difference results from their assumption that case isolation is absolutely effective, so an individual's "infectious period" lasts only until he or she is hospitalized. In contrast, our approach is to keep the biological phenomenon of infectiousness separate from the control-mediated phenomenon of transmission, leading to a longer total symptomatic period with transmission weighted by control parameters depending on case management practices.

Our model can still be consistent with the serial interval data presented by Lipsitch et al. (The serial interval is the time from onset of symptoms in an index case to onset of symptoms in a subsequent case infected by the index case. If the transmission rate is constant and the population is well-mixed, this equals the sum of the mean incubation period and the mean infectious period. The serial interval for SARS in Singapore before full-scale control policies were implemented was 10 days—subtracting the mean incubation period of 5 days yields the estimated 5-day infectious period.) Most simply, an exponentially-distributed period of uniform infectiousness with a mean duration of 5 days (as modelled by Lipsitch et al) could be approximated in our model by setting h_c=0.2 and κ=0, though in our model the tail of the distribution would be truncated by disease recovery. A more likely depiction of events in

Singapore would be a higher hospitalization rate and non-zero κ, such that the weighted mean of all infectious periods (before and after case isolation) was 5 days. By separating the biological and control-mediated aspects of transmission, our model naturally portrays this or any other control scenario.

We therefore wish to characterize the natural history of the disease accurately. The duration of hospitalization is a plausible surrogate for the symptomatic period, but for a disease as pathogenic as SARS it is likely to be an overestimate, since patients must recover from severe lung damage and are not discharged from hospital until several days after all symptoms are resolved (Lee et al 2003). The most direct measurement of SARS infectious periods are the viral load measurements of Peiris et al (2003), which show that mean viremia (for 75 patients) peaks roughly 10 days after onset of symptoms, and after 15 days has dropped below its level after 5 days of symptoms. This is attributed to onset of IgG seroconversion, which begins as early as 10 days after onset of symptoms (with mean of 20 days).

These results indicate that symptomatic periods in our model, as shown in Figure S4B, probably characterize the period of high infectiousness quite adequately. Should there be any inaccuracies, our strategy of considering scenarios with different values of R_0 would largely buffer the impact on our results, since reproductive numbers estimated for particular outbreaks can be compared to model epidemics with the same net growth rate. This would entail a slight skew in parameter values: for instance, if we had underestimated the duration of infectiousness, for each R_0 scenario we would overestimate the baseline transmission rate, β. Simulations would show slightly faster epidemic growth than is justified, and hence slightly greater reductions in efficacy due to delaying control measures. A change in β has no effect on the relative importance of different routes of transmission, however, or on the impacts of control measures focused on contact precautions versus case management. The major findings of this study therefore should be robust to misestimation of the distribution of symptomatic periods.

References not found in main text

Caswell, H. (2001) *Matrix Population Models*, 2nd ed. Sinauer, Sunderland MA.

Health Canada (2003) Summary of Severe Acute Respiratory Syndrome (SARS) Cases: Canada and International: April 29, 2003. Accessed online at http://www.hc-sc.gc.ca/pphb-dgspsp/sars-sras/eu-ae/sars20030429_e.html

Poutanen, S.M (and 19 others) (2003) Identification of severe acute respiratory syndrome in Canada. N Engl J Med **348**: 1995-2005.

Tsang, K.W. (and 15 others) (2003) A cluster of cases of severe acute respiratory syndrome in Hong Kong. N Engl J Med **348**: 1977-1985.

World Health Organization (2003b) Update 58 - First global consultation on SARS epidemiology, travel recommendations for Hebei Province (China), situation in Singapore. Accessed online at http://www.who.int/csr/sars/archive/2003_05_17/en/

Figure captions – Supplementary Information

Figure 5

Testing sensitivity to the absolute size of the system. Selected results are presented for both HCW and community pools ten-fold smaller than in the main text (HCW pool has 300 individuals and community pool has 10,000 individuals). For each figure, all parameter values other than population sizes are as described in the main text. (A) Analogue of Fig. 2D. (B) Analogue of Fig. 2F. (C) Analogue of Fig. 3B. (D) Analogues of pie-charts from Figs. 4A-B.

Figure 6

Testing sensitivity to the relative size of the HCW pool. Results are presented for a HCW pool of 1000 individuals (compared to 3000 throughout the main text), and community pool of 100,000 individuals. Again, all other parameters are as given in the main text. (A) Analogue of Fig. 2D. (B) Analogue of Fig. 2F. (C) Analogue of Fig. 3B. (D) Analogues of pie-charts from Figs. 4A-B.

Figure 7

Robustness of conclusions regarding sensitivity of R to transmission-reduction parameters. All details are as given in Fig. 2F except as noted. (A) No quarantine: q=0. (B) No quarantine, and limited case isolation: h_c=0.1, h_h=0.1, q=0. (C) Case management as in Fig. 2F, but R_0=5. Also note Figs. S1B and S2B, which show the insensitivity of these results to absolute and relative size of the two pools.

Figure 8

Distribution of (A) incubation periods and (B) symptomatic periods used in the model, each generated from 10,000 Monte Carlo simulations using the stage progression rules outlined in the text.

Figure 5

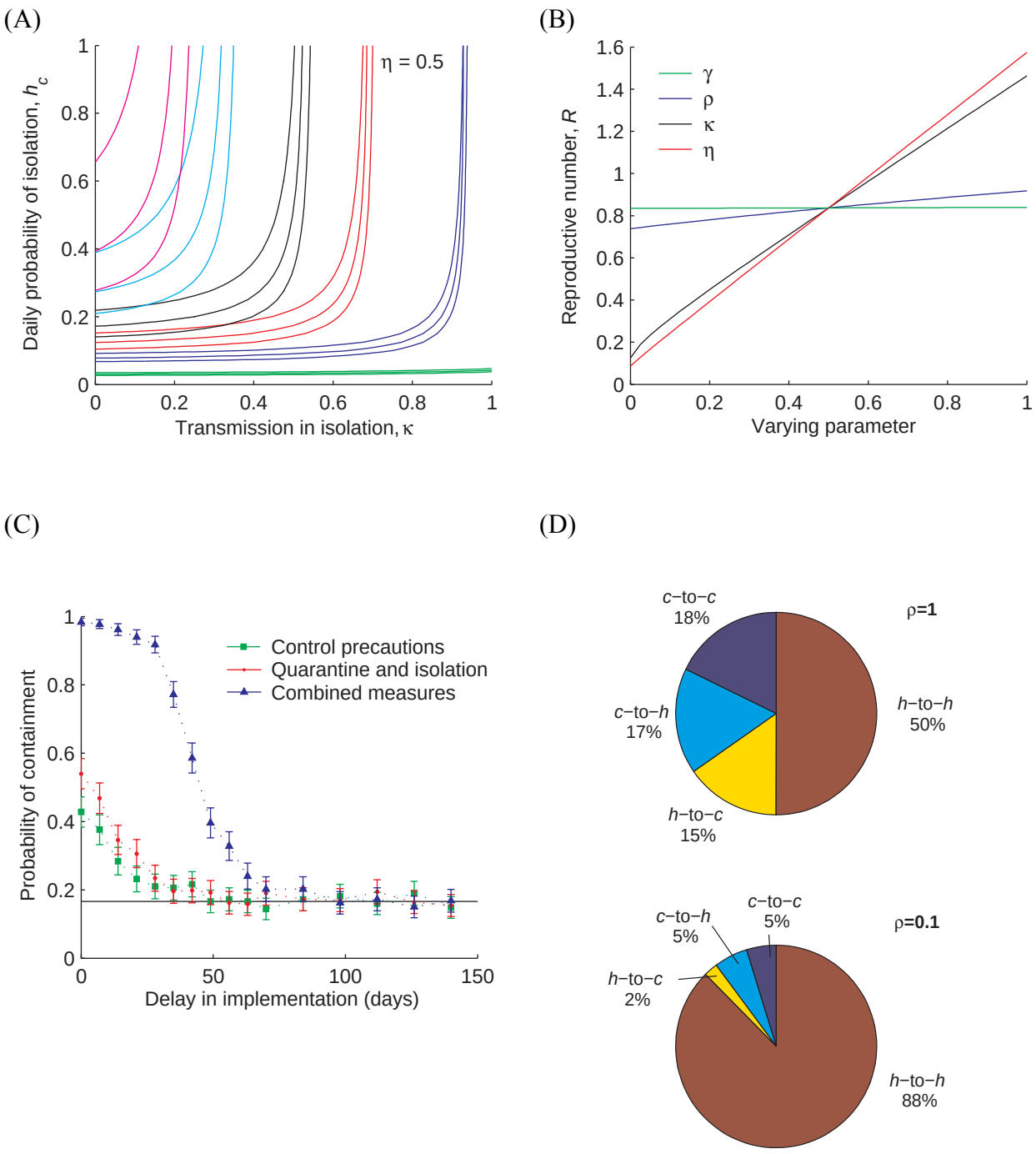
(A)
Daily probability of isolation, h_c
Transmission in isolation, κ
η = 0.5
(B)
Reproductive number, R
Varying parameter
γ
ρ
κ
η
(C)
Probability of containment
Delay in implementation (days)
Control precautions
Quarantine and isolation
Combined measures
(D)
c−to−c 18%
h−to−h 50%
c−to−h 17%
h−to−c 15%
ρ=1
c−to−h 5%
c−to−c 5%
h−to−c 2%
h−to−h 88%
ρ=0.1

Figure 6

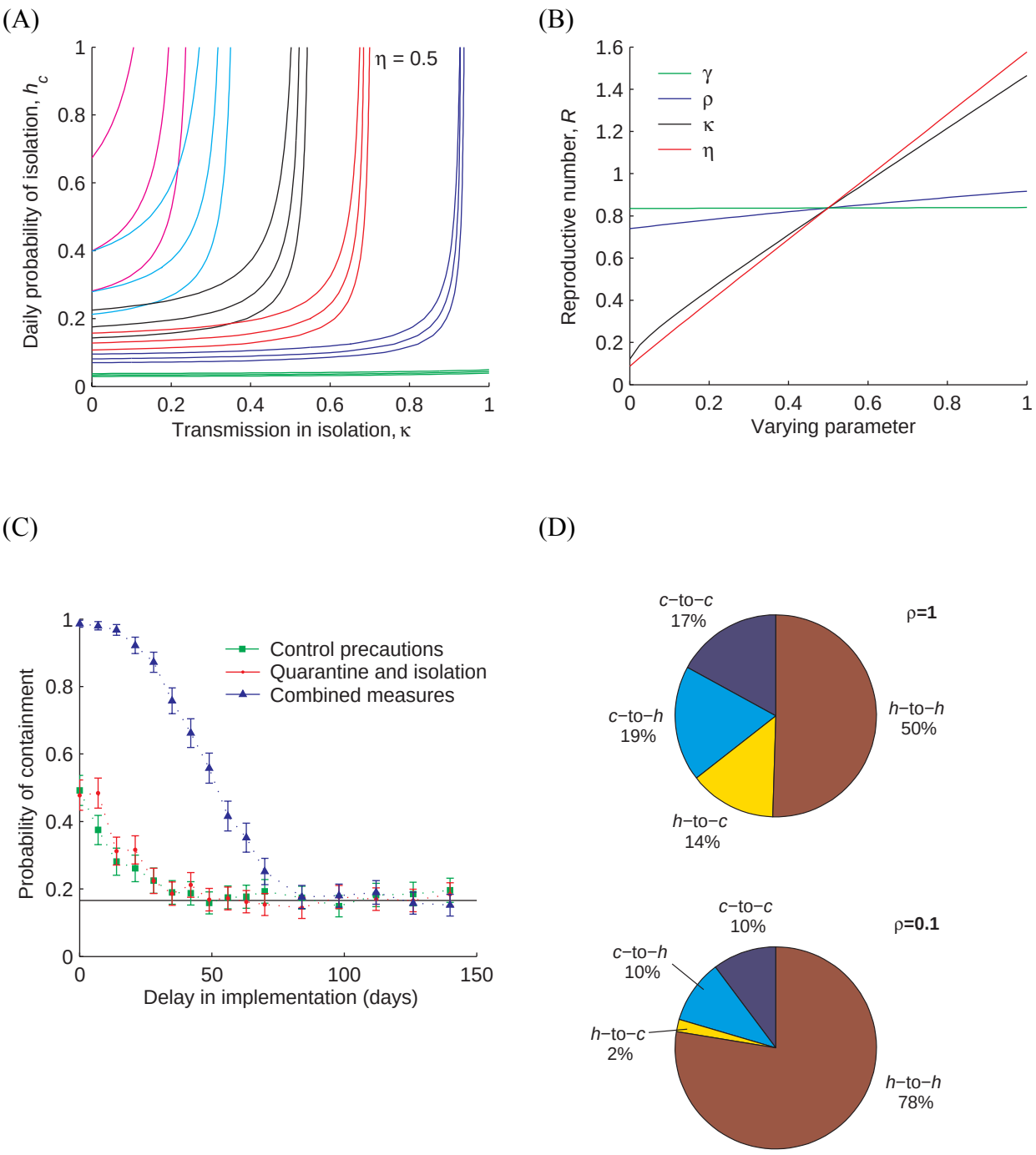
(A)
Daily probability of isolation, h_c
Transmission in isolation, κ
η = 0.5
(B)
Reproductive number, R
Varying parameter
γ
ρ
κ
η
(C)
Probability of containment
Delay in implementation (days)
Control precautions
Quarantine and isolation
Combined measures
(D)
c−to−c 17%
h−to−h 50%
c−to−h 19%
h−to−c 14%
ρ=1
c−to−c 10%
c−to−h 10%
h−to−c 2%
h−to−h 78%
ρ=0.1

Figure 7

(A)

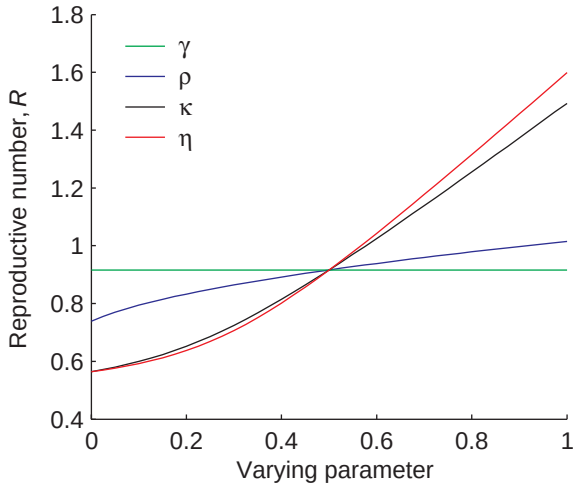
γ
ρ
κ
η
Reproductive number, R
Varying parameter
1.8
1.6
1.4
1.2
1
0.8
0.6
0.4
0
0.2
0.4
0.6
0.8
1

(B)

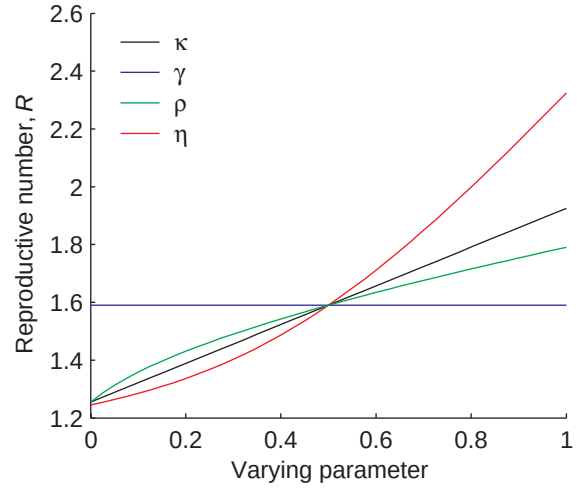
κ
γ
ρ
η
Reproductive number, R
Varying parameter
2.6
2.4
2.2
2
1.8
1.6
1.4
1.2
0
0.2
0.4
0.6
0.8
1

(C)

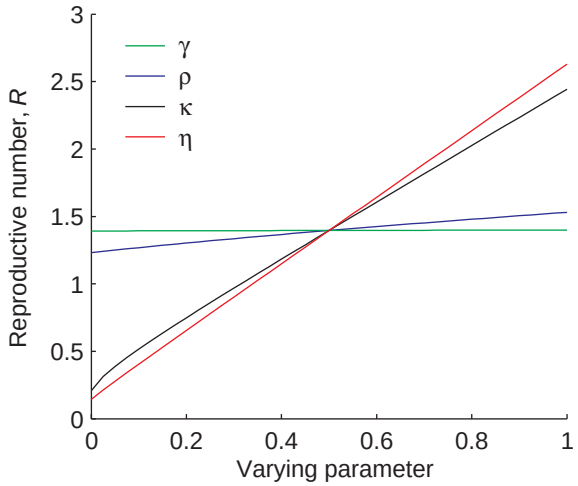
γ
ρ
κ
η
Reproductive number, R
Varying parameter
3
2.5
2
1.5
1
0.5
0
0
0.2
0.4
0.6
0.8
1

Figure 8

(A)

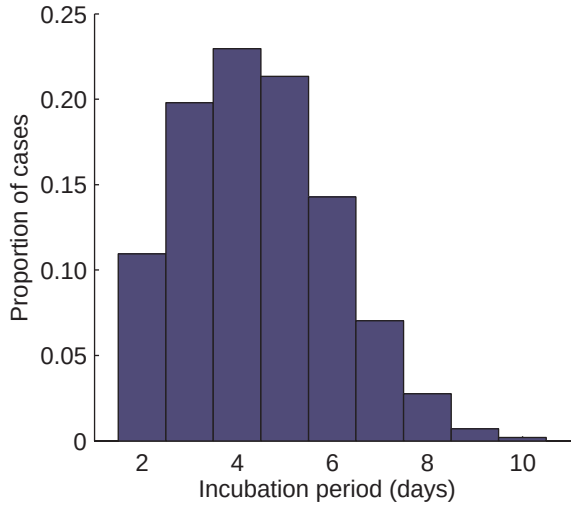
0.25
0.20
0.15
0.10
0.05
0
Proportion of cases
2
4
6
8
10
Incubation period (days)

(B)

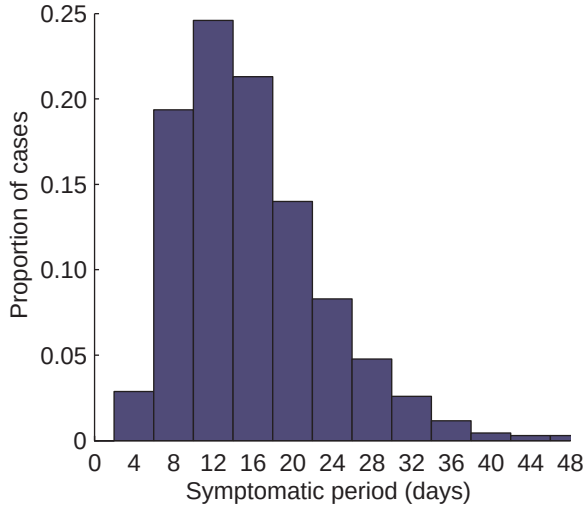
0.25
0.20
0.15
0.10
0.05
0
Proportion of cases
0
4
8
12
16
20
24
28
32
36
40
44
48
Symptomatic period (days)